Enhanced Brain Activation with Reduced Functional Connectivity in Stroke Patients: An EEG Study on Short-Term Working Memory

Haibin Xia[1], **Li Zhu**[2], **Lingmin Zhou**[3], **Feng Gao**[4], **Guifen Yang**[5], **Jiaru Dai**[6], **Lei Jin**[7] **& Wanzeng Kong**[18]
[1,2,3,6,7,8]School of Computer Science and Technology, Hangzhou Dianzi University, Hangzhou, Zhejiang, China
[4]School of Medicine, The Second Affiliated Hospital of Zhejiang University, Hangzhou, Zhejiang, China
[5]Tongde Hospital of Zhejiang Province, Hangzhou, Zhejiang, China

Abstract

While stroke rehabilitation emphasizes motor recovery, the neural mechanisms underlying short-term memory (STM) impairments—and corresponding compensatory processes—remain underexplored. This study investigates the neurodynamics of STM deficits by analyzing stage-specific brain activation and functional connectivity during perception and decision-making. Utilizing frequency-resolved electrophysiological measures, we identify a distinct dissociation in neural plasticity: increased theta-band power near lesion sites suggests adaptive compensation restoring global network efficiency, yet connectivity within core STM regions remains localized and weak, particularly during memory output. In contrast, higher-order cognitive deficits are marked by significant reductions in gamma-band power and network efficiency. By providing a stage-specific analysis of functional communication, this research pinpoints where compensatory efforts succeed or fail. Our findings offer a novel framework for understanding post-stroke plasticity limits and a targeted foundation for neuromodulatory interventions for cognitive recovery.

Keywords: Stroke, Short-term memory, Functional connectivity, Compensatory mechanisms, Electrophysiology

Introduction

Stroke remains a primary driver of global disability, imposing a substantial burden on public health (W. Johnson et al., 2016). While clinical interventions traditionally prioritize motor rehabilitation, the pervasive impact of post-stroke cognitive dysfunction is often underestimated, despite affecting up to 70% of survivors (Lugtmeijer et al., 2021). Among these deficits, short-term memory (STM) impairment acts as a critical bottleneck for functional independence. Unlike long-term memory (LTM), which is frequently preserved due to frontal sparing, STM relies heavily on posterior cortical regions that are highly vulnerable to stroke-induced disruption (Andrade et al., 2012; Nyberg et al., 2012). Since STM functions as the obligatory gateway for encoding novel information into LTM, its failure cascades into broader deficits, constraining ancillary domains such as language processing (Norris, 2017; Salis et al., 2015). Consequently, addressing STM decline is not merely a specific therapeutic target but a foundational requirement for broader cognitive recovery.

Dissecting the neural mechanisms of these impairments requires high-resolution temporal analysis. Electroencephalography (EEG) is particularly well-suited for this purpose, with established evidence linking theta and gamma oscillations to the core dynamics of memory encoding and retrieval (E. L. Johnson et al., 2020; Klimesch, 1996). Seminal research demonstrates that theta power, in particular, scales with cognitive load—mirroring hippocampal activity—while gamma rhythms facilitate local processing (Klimesch et al., 1997; Schack et al., 2002). However, a significant gap remains in current literature: existing studies predominantly focus on healthy populations or rely on single-channel spectral power attributes (Singh et al., 2015). This reductionist approach is insufficient for characterizing stroke pathology, as it overlooks the critical role of inter-regional communication.

Emerging evidence suggests that cognitive function, particularly working memory, is an emergent property of coordinated network integration rather than isolated local activity (Shirer et al., 2012). To capture the true extent of post-stroke deficits, it is essential to move beyond localized power analysis to the characterization of functional network topology. Graph-theoretical approaches, utilizing metrics such as Phase-Locking Value (PLV), offer a robust framework for quantifying phase synchronization and inter-regional interactions. By applying these network-level measures to the theta and gamma bands, we can effectively map the breakdown of functional connectivity and identify the compensatory reorganization mechanisms inherent to the post-stroke brain (Handayani et al., 2018; Zeng et al., 2022).

Building on these advancements, this study integrates phase-locking value network analysis with power spectral density analysis to conduct a comprehensive temporal and spatial examination of EEG data from stroke patients. This approach aims to uncover neural mechanisms underlying cognitive impairments, providing insights into the interplay between brain regions in this population. Specifically, we explore the underlying causes of short-term memory decline in stroke patients through a comparative analysis approach. By examining EEG activity during short-term memory tasks in both stroke patients and healthy controls, and further analyzing differences between lesion and non-lesion brain regions, the research aims to uncover the roles specific brain areas play in memory impairment. Identifying relevant biomarkers, this study seeks to provide targeted insights and strategies to support cognitive rehabilitation in stroke patients. The key contributions of this research include:

- Adapting the n-back paradigm to evaluate short-term memory perception in stroke patients and clinically col-

[1]Corresponding author(kongwanzeng@hdu.edu.cn).

In G. Boleda, I. Dautriche, M. Maldonado, C. Saldana and T. Torrent (Eds.), *Proceedings of the 48th Annual Conference of the Cognitive Science Society*

lecting comprehensive EEG datasets.

- Introducing a hybrid analytical framework that integrates power spectral density (PSD) and phase-locking value (PLV) to examine lesion effects and differentiate between the decoding and retrieval stages. This approach reveals heightened brain activation near lesions but reduced functional connectivity.
- Investigating the influence of lesion regions on short-term memory performance and uncovering compensatory mechanisms the brain employs to mitigate the impact of these lesions.

Material and Methods

Framework of Our Analysis Pipe

As illustrated in Fig. 1, our analytical framework spans the entire pipeline from experimental design to mechanistic exploration. Focusing on θ and γ oscillations, we analyzed neural dynamics through two complementary lenses: Power Spectral Density to map local spatial activation, and Phase Locking Value to reconstruct functional networks. Within these networks, the WKPN algorithm was employed to pinpoint critical hubs. By integrating these phase-based metrics across distinct task stages, we elucidated the specific inter-regional interactions that underpin short-term memory.

Experimental Design & Preprocessing

Participants and Experimental Protocol The study recruited 20 participants, comprising 10 stroke survivors (etiologies: hemorrhage, cerebral/lacunar infarction; mean disease duration: 15 months) and 10 healthy controls, under a protocol approved by the Ethics Committee of Tongde Hospital. To assess short-term memory while mitigating verbal processing demands and cognitive fatigue, we administered a modified 1-back paradigm using pictorial stimuli (Owen et al., 2005). The session consisted of 50 pseudo-randomized trials where participants identified immediate stimulus repetitions. During the task, EEG data were continuously acquired using a 64-channel wireless Neuracle system (sampling rate: 1000 Hz), with Ag/AgCl electrodes arranged according to the international 10-20 system (Ground: Fz).

Preprocessing EEG data were re-referenced to the common average and band-pass filtered between 0.05 and 50 Hz, with a notch filter applied to eliminate power line interference. Ocular artifacts were corrected using Independent Component Analysis (ICA) (Albera et al., 2012). The continuous data were then segmented into two distinct cognitive epochs relative to stimulus onset: an *input* phase (-2000 to 0 ms) and a *output* phase (2000 to 8000 ms). Spectral analyses focused on the θ (4–8 Hz) and γ (30–50 Hz) bands, following established protocols for STM assessment (Jones et al., 2020).

Power Spectrum Density Computing

In order to analyze the frequency characteristics of EEG data, the power spectrum is calculated through the following steps (Ahirwal & Londhe, 2012):

PSD Computing. The power spectral density was computed by squaring the magnitude of the Fourier coefficients and averaging the results over multiple epochs (Youngworth et al., 2005). The PSD, denoted as $P[k]$, quantifies the power of each frequency component and is given by:

$$P[k] = \frac{1}{N} |X[k]|^2, \tag{1}$$

where N represents the total number of samples. This calculation reveals the power distribution of the EEG signals across various frequency bands. Averaging over several epochs improves the reliability of the PSD estimate by minimizing the influence of transient artifacts and noise.

Normalization. To facilitate comparison and account for individual variability, the power values were normalized. This involved dividing the power within each frequency band by the total power across all bands, yielding relative power values. The normalized power $P_{\text{norm}}[k]$ is defined as:

$$P_{\text{norm}}[k] = \frac{P[k]}{\sum_{k=0}^{N-1} P[k]} \tag{2}$$

Normalization helps eliminate inter-subject differences in overall power, which can be influenced by factors like electrode impedance and scalp conductivity. By focusing on relative power, we can make more accurate comparisons of neural activity patterns across subjects and experimental conditions. The power spectrum computation offered valuable insights into the frequency characteristics of the EEG data, enabling the identification of dominant oscillatory patterns and their modulation under different experimental conditions. These frequency-domain features were essential for understanding the neural dynamics underlying cognitive processes and differentiating between various states of brain activity.

Functional Connectivity

Constructing Brain Network. The human brain can be understood as a complex network defined by intricate connectivity patterns. In our study, we focused on constructing brain networks based on PLV within the theta and gamma frequency bands. First, we extracted the data corresponding to these frequency bands from the epoch data. Following this, we utilized the Hilbert Transform to pairs of electrode signals $x(t)$ and $y(t)$ (Zhang et al., 2014), obtaining their analytic signals $z_x(t)$ and $z_y(t)$, as defined by the following equations.

$$\begin{aligned} z_x(t) &= x(t) + iHT(x(t)), \\ z_y(t) &= y(t) + iHT(y(t)) \end{aligned} \tag{3}$$

The relative phase $\Delta\phi(t)$ between $z_x(t)$ and $z_y(t)$ was also computed, and the corresponding PLV was calculated as (Celka, 2007),

$$PLV_{xy} = \left| \frac{1}{n} \sum_{k=1}^{n} e^{i\Delta\phi(t_k)} \right|, \tag{4}$$

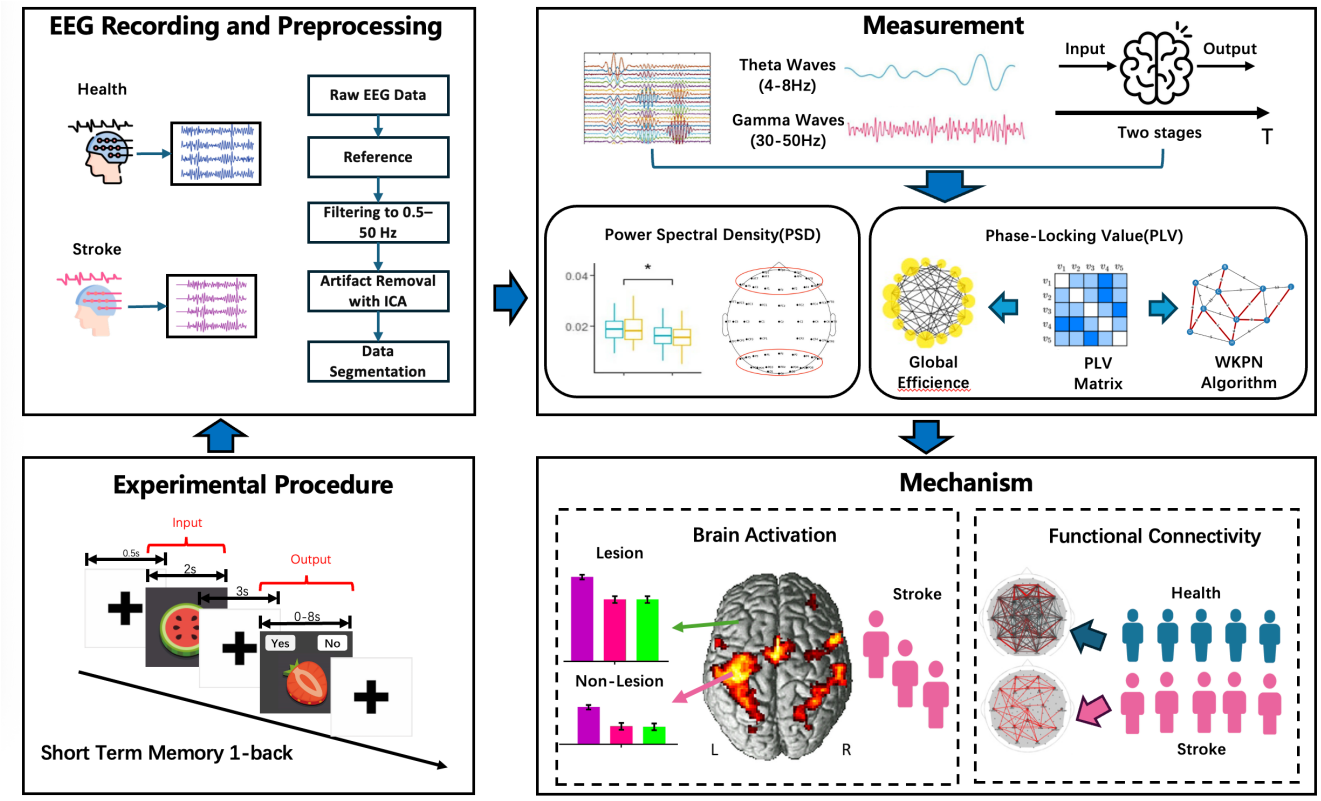

Figure 1: Framework of our analysis pipe

where n is the number of data points and t_k represents the time index. The resulting PLV ranges between 0 and 1. A higher PLV indicates stronger phase synchronization between the two signals, with a value of 1 signifying complete phase alignment of one signal with the other.

Network topology properties. To derive the connection weight matrix, we take the inverse of each element in the PLV matrix. This method decreases the distance between nodes with stronger connections, representing higher transmission efficiency. The calculation is expressed as:

$$d_{ij} = \frac{1}{PLV_{ij}}, \tag{5}$$

Using d_{ij}, we formed a brain connectivity computing with the 59 EEG electrodes, which removes the 5 functional electrodes. To characterize the connectivity of the network, we applied metrics like global efficiency. Global efficiency measures the efficiency of information transfer across the network and is defined as the inverse of the average shortest path length between any pair of nodes. This metric reflects the network's overall connectivity and capacity for information transfer, and is calculated as follows:

$$E_{global} = \frac{1}{n(n-1)} \sum_{i \neq j} \frac{1}{d_{ij}}, \tag{6}$$

Weighted K-Step Propagation Number (WKPN) Algorithm. To quantify the influence of specific EEG channels and lesion areas on global network cohesion, we employed the Weighted K-Step Propagation Number (WKPN) algorithm. Rooted in graph theory, this method evaluates node centrality by integrating topological structure with propagation efficiency. The implementation proceeds as follows:

First, based on the edge weights d_{ij} of the constructed brain network, we defined the shortest path distance $\text{dist}(v_i, v_j)$ between nodes v_i and v_j as the minimized sum of weights along the path:

$$\text{dist}(v_i, v_j) = \min \left(\sum_{(v_k, v_l) \in P_{ij}} d_{kl} \right), \tag{7}$$

where P_{ij} denotes the set of all possible paths connecting v_i and v_j.

Next, let d be the network diameter. For a given propagation radius $K \in [0, d]$, the K-step propagation number $N_{K_{v_i}}$ represents the count of nodes accessible from v_i within distance K. We then incorporated information entropy to derive the K-step structural entropy H^K of the entire network:

$$N_{K_{v_i}} = \left| \{ v_j \mid \text{dist}(v_i, v_j) \leq K \} \right| \tag{8}$$

$$H^K = -\sum_{i=1}^{n} \frac{N_{v_i}^K}{\sum_{j=1}^{n} N_{v_j}^K} \log \left(\frac{N_{v_i}^K}{\sum_{j=1}^{n} N_{v_j}^K} \right). \tag{9}$$

Finally, the global importance score Q_{v_i} for node v_i is aggregated across all steps from $K = 0$ to d. This metric balances the localized propagation capability with the global structural entropy:

$$Q_{v_i} = \sum_{K=0}^{d} \left(1 - \frac{H^K - \min(H)}{\max(H) - \min(H)}\right) \times \left(\frac{N_{v_i}^K - \min\left(N^K\right)}{\max\left(N^K\right) - \min\left(N^K\right)}\right), \tag{10}$$

where $H = \{H_0, \cdots, H_d\}$ and N^K represents the vector of propagation numbers at step K. By ranking nodes based on Q_{v_i}, we identified critical regions within the PLV-based brain network, leveraging the algorithm's validated robustness in complex system analysis.

Temporal Segmentation of Working Memory

To dissociate the temporal dynamics of memory processing, we operationalized the task into two functional stages aligned with the component process model (Rypma & D'Esposito, 2000): (1) the Input stage, defined as the initial 2000ms stimulus presentation window where sensory registration and maintenance occur; and (2) the Output stage, encompassing the subsequent period requiring memory readout and decision-making. This segmentation permits a granular analysis of stage-specific neural deficits, distinguishing between encoding failures and retrieval dysfunction.

Statistical Analysis.

Between-group differences in normalized PSD, mean PLV, global efficiency, and WKPN metrics were assessed using two-tailed independent-sample t-tests; within-patient stage and lesion–non-lesion contrasts were assessed using paired t-tests.

Results

Experiment 1: Brain Activation Revealed by Power Spectral Density Analysis in Stroke Patients and Healthy Controls

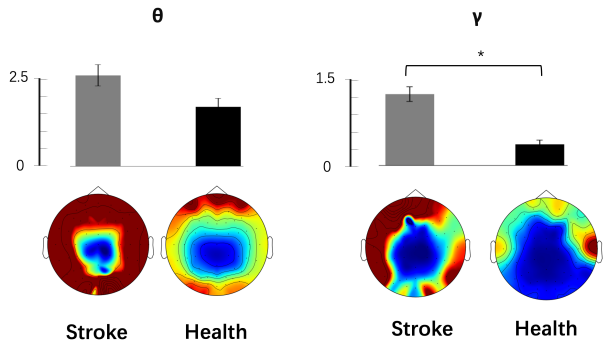

Figure 2: Grand average topographic maps of theta and gamma bands in healthy controls and stroke patients.

Fig. 2 presents group-averaged PSD topographies alongside quantitative power comparisons, revealing a frequency-dependent dissociation in neural reorganization. Globally, stroke patients exhibited elevated power across both theta and gamma bands, consistent with reports of pathological spectral upregulation (Xu et al., 2024), while maintaining the canonical 1/f power distribution. Spatially, however, distinct activation patterns emerged. In the theta band, cohort-wide analysis identified a subset of patients with abnormal energy surges concentrated specifically within lesion territories, suggesting a localized compensatory mechanism. In contrast, gamma activity displayed a globally altered spatial distribution relative to controls. These findings collectively highlight that post-stroke reorganization manifests through both global power amplification and regionally specific network alterations.

Experiment 2: The Two-Stage Mechanism of Brain Activation in Short-Term Memory Perception

Following normalization to control for inter-subject variability, statistical analysis confirmed a significant global upregulation of spectral power in stroke survivors compared to healthy controls across both input and output stages ($p < 0.05$). Specifically, the elevated theta power aligns with established markers of reduced vigilance (Kamzanova et al., 2014), suggesting that the post-stroke brain may resort to inefficient neural recruitment to maintain cognitive performance (Hanouneh et al., 2018).

Topographical statistical mapping (Fig. 3) further localized these spectral divergences. Significant group differences were predominantly clustered in the occipital cortex, reinforcing its critical role in visual STM processing. Crucially, a frequency-dependent spatial dissociation emerged: electrodes exhibiting significant deviations were notably more widespread in the gamma band than in the theta band.

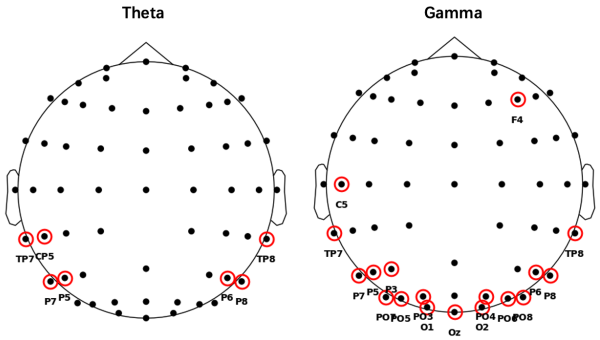

Figure 3: Electrode positions showing significant differences between health and stroke patients across two stages

This dissociation implies distinct pathological mechanisms. The widespread gamma alterations suggest that high-frequency local processing—essential for feature binding and sensory integration—is highly sensitive to post-stroke disruption. In contrast, the more focal theta differences may reflect specific, localized compensatory reorganization within the vi-

sual retention network. Collectively, these findings highlight the occipital cortex as a primary locus of dysfunction and suggest that gamma oscillations may serve as a more sensitive biomarker for network-wide cognitive integrity than theta rhythms.

Experiment 3: Functional Connectivity Revealed by PLV in Stroke Patients and Healthy Controls

We evaluated whole-brain integration capacity via Global Efficiency (E_{glob}) derived from PLV-based functional networks, revealing a marked frequency-dependent dissociation. While theta networks showed a non-significant trend toward increased efficiency in patients (0.57 vs. 0.52), gamma networks exhibited a significant reduction compared to controls (0.52 vs. 0.59, $p < 0.05$). This dissociation suggests that stroke selectively impairs high-frequency integration—critical for binding distributed information—while sparing or potentially reorganizing low-frequency substrates.

To validate the robustness of these topological findings, we analyzed network density across a continuous range of proportional thresholds (Fig. 4). Consistent with efficiency metrics, theta connectivity remained indistinguishable between groups. Conversely, stroke survivors displayed profound gamma hypoconnectivity, retaining significantly fewer functional edges than controls regardless of the threshold applied. This stability confirms that the gamma efficiency deficit stems from a widespread loss of functional connections rather than arbitrary thresholding effects.

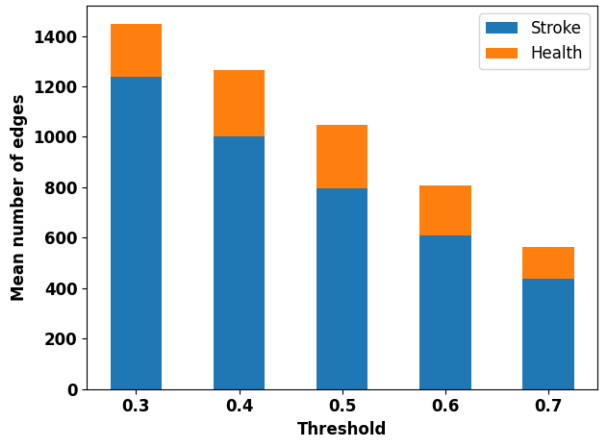

Figure 4: The number of gamma band PLV edges across different thresholds

To elucidate the nodal hierarchy driving these topological shifts, we applied the WKPN algorithm to map critical network hubs (Fig. 5). A distinct frequency-dependent dissociation emerged. The patient gamma network exhibited a profound collapse of functional integration, characterized by significantly reduced connectivity and global efficiency. This breakdown suggests that stroke selectively disrupts the fast, local synchronization mechanisms essential for feature binding, thereby hindering the complex cognitive processing reliant on high-frequency communication.

In stark contrast, the theta band demonstrated remarkable topological resilience. Despite the presence of focal lesions, global efficiency in patients remained statistically comparable to that of healthy controls. Crucially, this preservation was mediated by a reorganization of connectivity pathways—specifically, the emergence of alternative long-range coupling between frontal and occipital regions. These findings suggest a compensatory strategy where the post-stroke brain actively reroutes information via low-frequency channels to bypass the functional fragmentation of high-frequency networks, maintaining a baseline of integrative capacity.

Experiment 4: The Two-Stage Mechanism of Functional Connectivity in Short-Term Memory Perception

To verify the temporal stability of these network alterations, we segmented the analysis into input and output stages. Temporal segmentation analysis confirmed the robustness of frequency-dependent network alterations. Stroke patients consistently exhibited reduced gamma-band global efficiency ($p < 0.05$) alongside elevated theta efficiency, regardless of task phase. This establishes that disrupted high-frequency integration is a stable, load-independent trait of the post-stroke brain.

Crucially, nodal centrality revealed a stage-dependent "offloading" mechanism within the theta band. Functional reliance shifted significantly from lesion to non-lesion substrates, with lesion node importance declining from the input to the output stage ($p < 0.05$). This suggests that while compromised regions may support initial sensory registration, the network actively bypasses them during decision-making to preserve cognitive performance.

Building on the significant PSD differences observed in frontal and occipital regions—key hubs for short-term memory—we conducted a targeted subnetwork analysis of mean PLV (Fig. 6). This revealed selective connectivity deficits: patients showed significantly reduced PLV compared to controls within the occipital subnetwork (both theta and gamma bands) and in long-range fronto-occipital connections (gamma band, $p < 0.05$). No significant differences were found in other subnetworks. These findings underscore a selective vulnerability in post-stroke architecture: the disease primarily compromises local occipital processing and high-frequency cross-regional integration, thereby impairing visual and higher-order cognitive functions while sparing other network components.

Disscussion

Frequency-dependent Compensatory Mechanisms and Network Reorganization

The present study reveals a distinct frequency-dependent dissociation in post-stroke neural reorganization. The observed elevation in theta band power near lesion sites, cou-

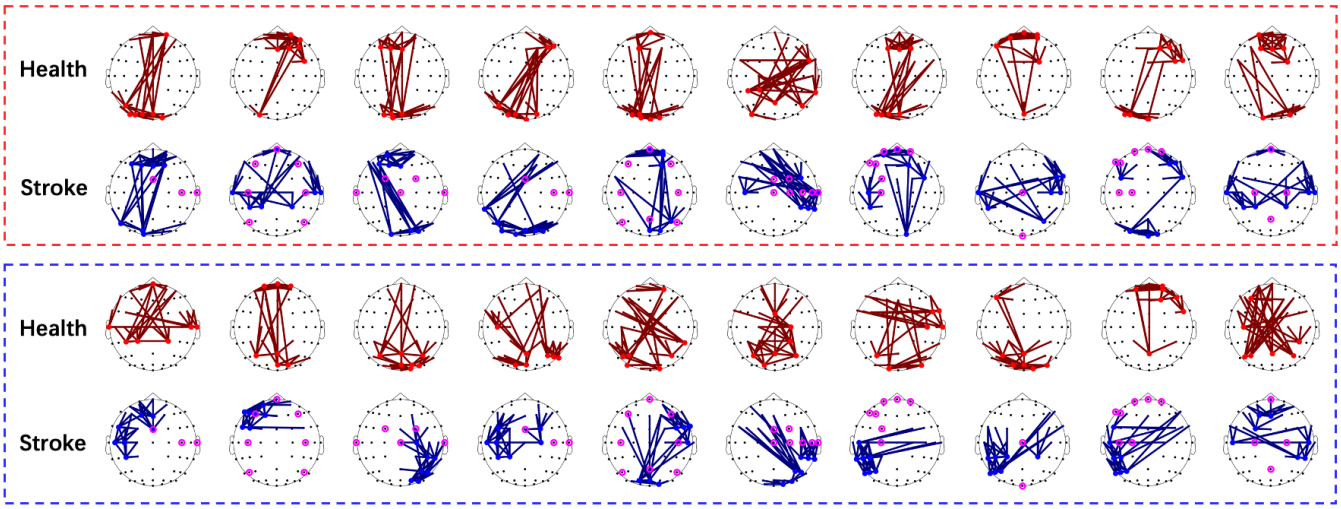

Figure 5: The top seven nodes in the θ and γ band ranked by importance using the WKPN algorithm, along with the five strongest connections for each node

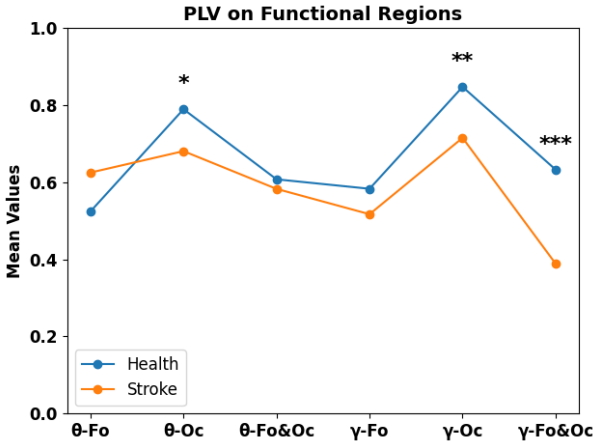

Figure 6: Comparison of mean PLV in theta and gamma bands in memory-related brain regions (Frontal and Occipital)

pled with preserved global network efficiency, points to a localized compensatory process. This adaptation appears to support foundational cognitive functions such as attention and information registration, aligning with the role of theta oscillations in organizing cognitive resources (Sauseng et al., 2010). In contrast, the gamma band exhibited a significant decline in both power and global efficiency. Since gamma oscillations are critical for rapid information integration and cross-regional communication (Fitzgibbon et al., 2004), this deficit reflects a weakened capacity for maintaining the complex neural synchronization required for short-term memory. The results suggest that while the post-stroke brain effectively recruits low-frequency networks to maintain baseline function, it fails to sustain the high-frequency coherence necessary for advanced information processing.

Stage-Specific Dynamics and Connectivity Deficits

Nodal analysis reveals that the impact of structural damage is temporally specific. Lesion regions exerted a significantly stronger influence on network topology during the output stage relative to the input stage. This implies that while sensory registration remains relatively robust, executive decision-making and recall processes are disproportionately compromised by lesion-induced perturbations. Anatomically, this deficit is characterized by weakened fronto-occipital connectivity. Furthermore, the dissociation between elevated theta synchronization (linked to preserved long-term retrieval) and suppressed gamma connectivity (underlying short-term memory deficits) supports the hypothesis that stroke selectively impairs the active maintenance of novel information while leaving consolidated knowledge structures relatively intact.

Conclusion

This study elucidates the neurodynamics of short-term memory impairments in stroke patients by integrating analyses of spectral power, functional connectivity, and inter-regional information exchange. We specifically targeted potential compensatory remodeling surrounding lesion territories. A distinct frequency-dependent dissociation emerged: In the theta band, patients exhibited focal power surges near lesion sites and preserved global network efficiency, suggesting an adaptive reorganization. However, connectivity within core STM nodes remained compromised—particularly during the memory output stage—indicating that this compensation is functionally incomplete. Conversely, the gamma band displayed widespread reductions in both power and efficiency, reflecting a breakdown in higher-order cognitive integration. These findings delineate the limits of post-stroke plasticity and provide a critical neurophysiological foundation for developing targeted STM rehabilitation interventions.

Acknowledgments

We extend our gratitude to all the authors for their invaluable contributions to the preparation of this manuscript. Additionally, we deeply appreciate the participation and cooperation of the subjects involved in this study.

References

Ahirwal, M. K., & Londhe, N. (2012). Power spectrum analysis of eeg signals for estimating visual attention. *International Journal of computer applications*, *42*(15), 22–25.

Albera, L., Kachenoura, A., Comon, P., Karfoul, A., Wendling, F., Senhadji, L., & Merlet, I. (2012). Ica-based eeg denoising: A comparative analysis of fifteen methods. *Bulletin of the Polish Academy of Sciences: Technical Sciences*, *60*(3 Special issue on Data Mining in Bioengineering), 407–418.

Andrade, S. P. C. d., Brucki, S. M. D., Bueno, O. F. A., & Siqueira Neto, J. I. (2012). Neuropsychological performance in patients with subcortical stroke. *Arquivos de Neuro-Psiquiatria*, *70*, 341–347.

Celka, P. (2007). Statistical analysis of the phase-locking value. *IEEE Signal Processing Letters*, *14*(9), 577–580.

Fitzgibbon, S., Pope, K., Mackenzie, L., Clark, C., & Willoughby, J. (2004). Cognitive tasks augment gamma eeg power. *Clinical neurophysiology*, *115*(8), 1802–1809.

Handayani, N., Haryanto, F., Khotimah, S. N., Arif, I., & Taruno, W. P. (2018). Coherence and phase synchrony analyses of eeg signals in mild cognitive impairment (mci): A study of functional brain connectivity. *Polish Journal of Medical Physics and Engineering*, *24*(1), 1–9.

Hanouneh, S., Amin, H. U., Saad, N. M., & Malik, A. S. (2018). Eeg power and functional connectivity correlates with semantic long-term memory retrieval. *Ieee Access*, *6*, 8695–8703.

Johnson, E. L., Kam, J. W., Tzovara, A., & Knight, R. T. (2020). Insights into human cognition from intracranial eeg: A review of audition, memory, internal cognition, and causality. *Journal of neural engineering*, *17*(5), 051001.

Johnson, W., Onuma, O., Owolabi, M., & Sachdev, S. (2016). Stroke: A global response is needed. *Bulletin of the World Health Organization*, *94*(9), 634.

Jones, K. T., Johnson, E. L., & Berryhill, M. E. (2020). Frontoparietal theta-gamma interactions track working memory enhancement with training and tdcs. *Neuroimage*, *211*, 116615.

Kamzanova, A. T., Kustubayeva, A. M., & Matthews, G. (2014). Use of eeg workload indices for diagnostic monitoring of vigilance decrement. *Human factors*, *56*(6), 1136–1149.

Klimesch, W. (1996). Memory processes, brain oscillations and eeg synchronization. *International journal of psychophysiology*, *24*(1-2), 61–100.

Klimesch, W., Doppelmayr, M., Schimke, H., & Ripper, B. (1997). Theta synchronization and alpha desynchronization in a memory task. *Psychophysiology*, *34*(2), 169–176.

Lugtmeijer, S., Lammers, N. A., de Haan, E. H., de Leeuw, F.-E., & Kessels, R. P. (2021). Post-stroke working memory dysfunction: A meta-analysis and systematic review. *Neuropsychology review*, *31*, 202–219.

Norris, D. (2017). Short-term memory and long-term memory are still different. *Psychological bulletin*, *143*(9), 992.

Nyberg, L., Lövdén, M., Riklund, K., Lindenberger, U., & Bäckman, L. (2012). Memory aging and brain maintenance. *Trends in cognitive sciences*, *16*(5), 292–305.

Owen, A. M., McMillan, K. M., Laird, A. R., & Bullmore, E. (2005). N-back working memory paradigm: A meta-analysis of normative functional neuroimaging studies. *Human brain mapping*, *25*(1), 46–59.

Rypma, B., & D'Esposito, M. (2000). Isolating the neural mechanisms of age-related changes in human working memory. *Nature neuroscience*, *3*(5), 509–515.

Salis, C., Kelly, H., & Code, C. (2015). Assessment and treatment of short-term and working memory impairments in stroke aphasia: A practical tutorial. *International Journal of Language & Communication Disorders*, *50*(6), 721–736.

Sauseng, P., Griesmayr, B., Freunberger, R., & Klimesch, W. (2010). Control mechanisms in working memory: A possible function of eeg theta oscillations. *Neuroscience & Biobehavioral Reviews*, *34*(7), 1015–1022.

Schack, B., Vath, N., Petsche, H., Geissler, H.-G., & Möller, E. (2002). Phase-coupling of theta–gamma eeg rhythms during short-term memory processing. *International Journal of Psychophysiology*, *44*(2), 143–163.

Shirer, W. R., Ryali, S., Rykhlevskaia, E., Menon, V., & Greicius, M. D. (2012). Decoding subject-driven cognitive states with whole-brain connectivity patterns. *Cerebral cortex*, *22*(1), 158–165.

Singh, Y., Singh, J., Sharma, R., & Talwar, A. (2015). Fft transformed quantitative eeg analysis of short term memory load. *Annals of neurosciences*, *22*(3), 176.

Xu, M., Zhang, Y., Zhang, Y., Liu, X., & Qing, K. (2024). Eeg biomarkers analysis in different cognitive impairment after stroke: An exploration study. *Frontiers in Neurology*, *15*, 1358167.

Youngworth, R. N., Gallagher, B. B., & Stamper, B. L. (2005). An overview of power spectral density (psd) calculations. *Optical manufacturing and testing VI*, *5869*, 206–216.

Zeng, H., Jin, Y., Wu, Q., Pan, D., Xu, F., Zhao, Y., Hu, H., & Kong, W. (2022). Eeg-fcv: An eeg-based functional connectivity visualization framework for cognitive state evaluation. *Frontiers in Psychiatry*, *13*, 928781.

Zhang, J., Wang, N., Kuang, H., & Wang, R. (2014). An improved method to calculate phase locking value based on hilbert–huang transform and its application. *Neural Computing and Applications*, *24*, 125–132.